A high-sensitivity laboratory system for measuring the microwave properties of gases under simulated conditions for planetary atmospheres

Thomas R. Hanley[1] and Paul G. Steffes[1]

Received 12 May 2007; revised 5 September 2007; accepted 25 September 2007; published 25 December 2007.

[1] A system for measuring the microwave properties of gases under simulated conditions for planetary atmospheres has been under continuous development at Georgia Tech for over 2 decades (see, e.g., DeBoer and Steffes, 1996). The measurements from this system form the basis for accurately modeling the microwave properties of gases under various planetary conditions, which are essential in determining the presence and concentration of such gases through various microwave remote sensing techniques. This system consists of two independent configurations, one capable of measuring gas mixtures up to pressures of 3 bars at frequencies from 22 to 40 GHz, and another capable of pressures up to 12 bars over the frequency range from 1.5 to 24.1 GHz. The former configuration exhibits maximum 2-σ sensitivities in absorptivity of 0.25 dB/km and in refractivity of 2.0, while the latter configuration exhibits maximum 2-σ sensitivities in absorptivity ranging from 0.01 dB/km at 1.5 GHz (20 cm) to 1.0 dB/km at 24.1 GHz (1.25 cm) and in refractivity from 0.05 at 1.5 GHz to 3.13 at 24.1 GHz.

Citation: Hanley, T. R., and P. G. Steffes (2007), A high-sensitivity laboratory system for measuring the microwave properties of gases under simulated conditions for planetary atmospheres, *Radio Sci.*, *42*, RS6010, doi:10.1029/2007RS003693.

1. Introduction

[2] Radio absorptivity data for planetary atmospheres obtained from spacecraft radio occultation experiments, entry probe radio signal absorption measurements, and earth-based or spacecraft-based radio astronomical (emission) observations can be used to infer abundances of microwave absorbing constituents in those atmospheres, as long as reliable information regarding the microwave absorbing properties of potential constituents is available. The use of theoretically derived microwave absorption properties for such atmospheric constituents, or the use of laboratory measurements of such properties taken under environmental conditions that are significantly different than those of the planetary atmosphere being studied, often leads to considerable misinterpretation of available opacity data. For example, laboratory measurements completed by *Hoffman et al.* [2001] showed that the centimeter-wavelength opacity from gaseous phosphine (PH_3) under simulated conditions for the outer planets varied significantly from that predicted by theory over a wide range of temperatures and pressures. These results have directly impacted planning and scientific results from the study of Saturn's atmosphere with the Cassini Radio Science Experiment [see, e.g., *Mohammed*, 2005]. The recognition of the need to make such laboratory measurements of simulated planetary atmospheres over a range of temperatures and pressures which correspond to the altitudes probed by radio occultation experiments, entry probe radio link experiments, and radio astronomical observations, and over a range of frequencies which correspond to those used in both spacecraft experiments and in radio astronomical observations, has led to the development of a facility at Georgia Tech which is capable of making such measurements.

[3] The current high-sensitivity microwave measurement system at the Planetary Atmospheres Lab of the Georgia Institute of Technology is based on that described previously by *DeBoer and Steffes* [1996], *Kolodner and Steffes* [1998], *Hoffman et al.* [2001], and *Hanley and Steffes* [2005], along with the added ability to characterize and compensate for molecules that selectively adsorb or adhere to the surfaces in the system. This laboratory system allows characterization of the refractive and absorptive microwave properties of various gases and gas mixtures under certain temperature and

[1]School of Electrical and Computer Engineering, Georgia Institute of Technology, Atlanta, Georgia, USA.

0048-6604/07/2007RS003693

pressure conditions found in the atmospheres of our solar system's planets. The data retrieved from these measurements is useful in constructing models for the microwave and millimeter-wave absorption coefficients of gases as a function of frequency, temperature, pressure, and concentration. These models then allow researchers to retrieve planetary atmospheric compositions remotely through spacecraft radio occultations, entry probe radio link intensity measurements, or passive radiometric emission measurements.

[4] In the case of radio occultations (e.g., Cassini or Voyager), a carrier wave signal is transmitted through various altitudes of a planet's atmosphere in either an uplink or downlink configuration, usually across multiple frequency bands, between the spacecraft and earth as the spacecraft moves behind the planet. For entry probe radio links (e.g., Galileo) the transmission occurs between the entry probe and a nearby orbiting spacecraft. In the case of thermal emission measurements, the planet's blackbody radiation acts as a full-band transmitter. After precisely measuring the drop in signal intensity and phase caused by atmospheric attenuation and refraction, researchers can compare the results with the known properties of gases and retrieve temperature-pressure profiles and atmospheric composition. The accuracy of these retrievals not only depends on the measurement abilities of the spacecraft and earth stations, but also on the knowledge of the microwave and millimeter-wave properties of the gases present. Being able to more accurately measure those properties in a laboratory setting allows for more accurate scientific retrievals and knowledge of the composition, function, and formation of our solar system. This paper describes the latest equipment and procedures used in measuring and calculating the absorption and refraction of a gas or gas mixture.

2. Measurement Theory

[5] The method used to measure the microwave absorptivity of a gas is based on the lessening in the quality factor (Q) of a resonant mode of a cavity in the presence of a lossy gas. The technique of monitoring the changes of Q of different resonances of a cavity resonator in order to determine the refractive index and the absorption coefficient of an introduced gas or gas mixture (at those resonant frequencies) has been used for over one half of a century [see, e.g., *Bleaney and Loubser*, 1950; *Ho et al.*, 1966; *Morris and Parsons*, 1970; *Steffes and Eshleman*, 1981].

[6] The Q of a resonance is a unitless quantity defined as [*Matthaei et al.*, 1980]

$$Q = \frac{2\pi f_0 \times \text{Energy Stored}}{\text{Average Power Loss}} \tag{1}$$

where f_0 is the frequency of the resonance and can be measured directly as the frequency divided by its half-power bandwidth (f_0/BW). The opacity or absorptivity (α) of a gas is related to the Q of that gas by

$$\alpha = \frac{\varepsilon''\pi}{\varepsilon'\lambda} = \frac{1}{Q_{\text{gas}}}\frac{\pi}{\lambda}(\text{Nepers/km}), \tag{2}$$

where ε' and ε'' represent the real and imaginary permittivity of the gas and λ is the wavelength in km. The quality factor of a resonator loaded with a test gas can be represented by

$$\frac{1}{Q^m_{\text{loaded}}} = \frac{1}{Q_{\text{gas}}} + \frac{1}{Q_{\text{vac}}} + \frac{1}{Q_{\text{ext1}}} + \frac{1}{Q_{\text{ext2}}}, \tag{3}$$

where $Q^{\text{m}}_{\text{loaded}}$ is the measured quality factor of the gas filled resonator, Q_{gas} is the quality factor of the gas itself, Q_{vac} is the quality factor of the evacuated cavity resonator, and Q_{ext1} and Q_{ext2} represent the external coupling losses from the antenna probes in the resonator. Since only symmetric resonators are used, we can assume $Q_{\text{ext1}} = Q_{\text{ext2}}$. The Q_{ext} value can be calculated by measuring the transmissivity of the system, $t = 10^{-S/10}$ where S is the insertion loss of the resonator in decibels at the frequency of a particular resonance, and using the relations [*Matthaei et al.*, 1980]

$$\text{t} = \left[2\frac{Q^m}{Q_{ext}}\right]^2, \tag{4}$$

$$Q_{ext} = \frac{2Q^m}{\sqrt{t}}, \tag{5}$$

where Q^m represents a measured quality factor. Substitution of (5) into (3) yields

$$\frac{1}{Q_{gas}} = \frac{1-\sqrt{t_{loaded}}}{Q^m_{loaded}} - \frac{1-\sqrt{t_{vac}}}{Q^m_{vac}}, \tag{6}$$

with t_{loaded} and t_{vac} representing the transmissivities of the loaded and vacuum measurements, respectively. Calculating Q_{gas} in this manner is slightly flawed, however, as this formula does not account for changes in the center frequency of a resonance when a gas is present. If measurements are conducted under relatively benign conditions, (e.g., 270 K–400 K), it is possible to construct a tunable resonator which can be retuned to the original resonant frequency when the test gas is present [see, e.g., *Ho et al.*, 1966; *Morris and Parsons*, 1970]. However, under conditions of extreme temperature and pressure it is very hard to construct reliable tunable resonators. If "fixed-tuned" resonators are used, the frequency shift, which accompanies the introduction of the gas under test, changes the coupling of the resonator

and consequently the quality factor, even in the absence of opacity. Even if tunable resonators are used, the refractive effects of the gas under test can cause changes in coupling to the resonator, affecting the measured quality factor [*Morris and Parsons*, 1970]. Known as dielectric loading (described in more detail by *Spilker* [1990] and *Joiner* [1991]), this effect requires additional measurements of the quality factor and transmissivity of a resonance to be made in the presence of a lossless gas exhibiting the same refractive index as that of the gas under test. Using this measurement in place of that made under vacuum conditions in (6), substituting into (2), and converting from Nepers/km to dB/km (1 Np/km = 2 optical depths/km = 2*10 $\log_{10}$e (≈8.686) dB/km) gives the final formula for calculating absorptivity

$$\alpha = 8.686\frac{\pi}{\lambda}\left(\frac{1-\sqrt{t}_{\text{loaded}}}{Q^{\text{m}}_{\text{loaded}}} - \frac{1-\sqrt{t}_{\text{matched}}}{Q^{\text{m}}_{\text{matched}}}\right)\frac{\text{dB}}{\text{km}} \quad (7)$$

[*DeBoer and Steffes*, 1994].

[7] Measuring the refractivity of a gas is more direct than determining its opacity. Refractivity (N) is calculated as:

$$N = 10^6\frac{(f_{\text{vac}} - f_{\text{gas}})}{f_{\text{gas}}} \quad (8)$$

where f_{vac} and f_{gas} represent the center frequencies of a resonance measured with the system under vacuum and filled with the test gas mixture, respectively [*Tyler and Howard*, 1969]. This represents the refractivity of the entire gas mixture, which is the sum of the constituents' refractivities weighted by their mole fractions. Refractivity is dependent on pressure and temperature and is often presented in a normalized form to exclude these dependencies. Normalized refractivity is calculated as:

$$N' = \frac{NRT}{P}\left(\frac{N - units \times cm^3}{molecule}\right) \quad (9)$$

where T is the temperature in Kelvin, P is the pressure in atmospheres and R = 1.362344 × 10^{-22} (atm*cm^3)/(molecule*K).

[8] Although its value is not directly used in calculating absorption or refraction, knowing the asymmetry of a particular resonance is helpful in determining whether a resonance is corrupted by overlapping resonances of lower Qs and in calculating the corresponding measurement uncertainty. Asymmetry (A) can be defined as [*DeBoer and Steffes*, 1996]:

$$A = 100\frac{(f_h - f_c) - (f_c - f_l)}{(f_h - f_l)}\% \quad (10)$$

with f_h, f_l, and f_c, representing the higher frequency −3 dB point, lower frequency −3 dB point, and center frequency of the resonance, respectively. Since two overlapping resonant modes might broaden disproportionately and give inaccurate results, only resonances with a low asymmetry (typically less than 5%) are used.

3. System Description

[9] The current measurement system configuration in use at Georgia Tech is shown in Figure 1. It is comprised of three major parts: the planetary atmospheric simulator, the microwave measurement subsystem, and the data handling subsystem.

3.1. Planetary Atmospheric Simulator

[10] The planetary atmospheric simulator controls and monitors the environment experienced by the microwave resonators, including the temperature and pressure conditions for the gas under test. The main component of the atmospheric simulator is a pressure vessel capable of handling pressures from vacuum to 12 atm with a volume of approximately 31 L. The vessel is cylindrical and made of stainless steel with a detachable top plate sealed by a Viton O-ring and vacuum grease. The top is bolted to the bottom with eight 1″ diameter bolts connected through unthreaded holes to washers and nuts and eight 3/8″ bolts that are threaded into the bottom flange. Gases are fed into the vessel through a series of regulators and valves. All components in the gas handling subsystem are connected with seamless 3/8″ outer diameter stainless steel tubing and Swagelok® fittings. The pressure vessel itself is contained in a temperature chamber. For temperatures between 173 K and 218 K, the temperature chamber is a Revco ultra-low temperature freezer. At warmer temperatures between room temperature and 550 K, the vessel is placed in a digitally controlled electric oven. The temperature inside the pressure vessel is monitored by an Omega® Model HH21 Microprocessor Thermometer connected to a T-type thermocouple probe inserted into a sealed and capped inverted 3/8″ outer diameter pipe protruding into the vessel, but not in direct contact with the gases inside. The thermometer has a resolution of 0.1° and a 3-σ accuracy of 0.3% of the displayed value ±0.6°C at temperatures below 0°C and 0.1% ± 0.6°C at temperatures above 0°C and the thermocouple has an accuracy of 1.0°C or 0.75% of the reading, whichever is greater. Positive pressures in the system are measured by an Omega® DPG7000 Digital Test Gauge with a resolution of 1 mbar and a 3-σ accuracy of 10 mbar, capable of measuring pressures up to 300 psi above ambient, whereas pressures below ambient are measured by a Hastings Model 760 vacuum gauge with a resolution of 1 torr and an accuracy of 1 mbar. For cross-correlation, absolute pressures between two bars and vacuum are

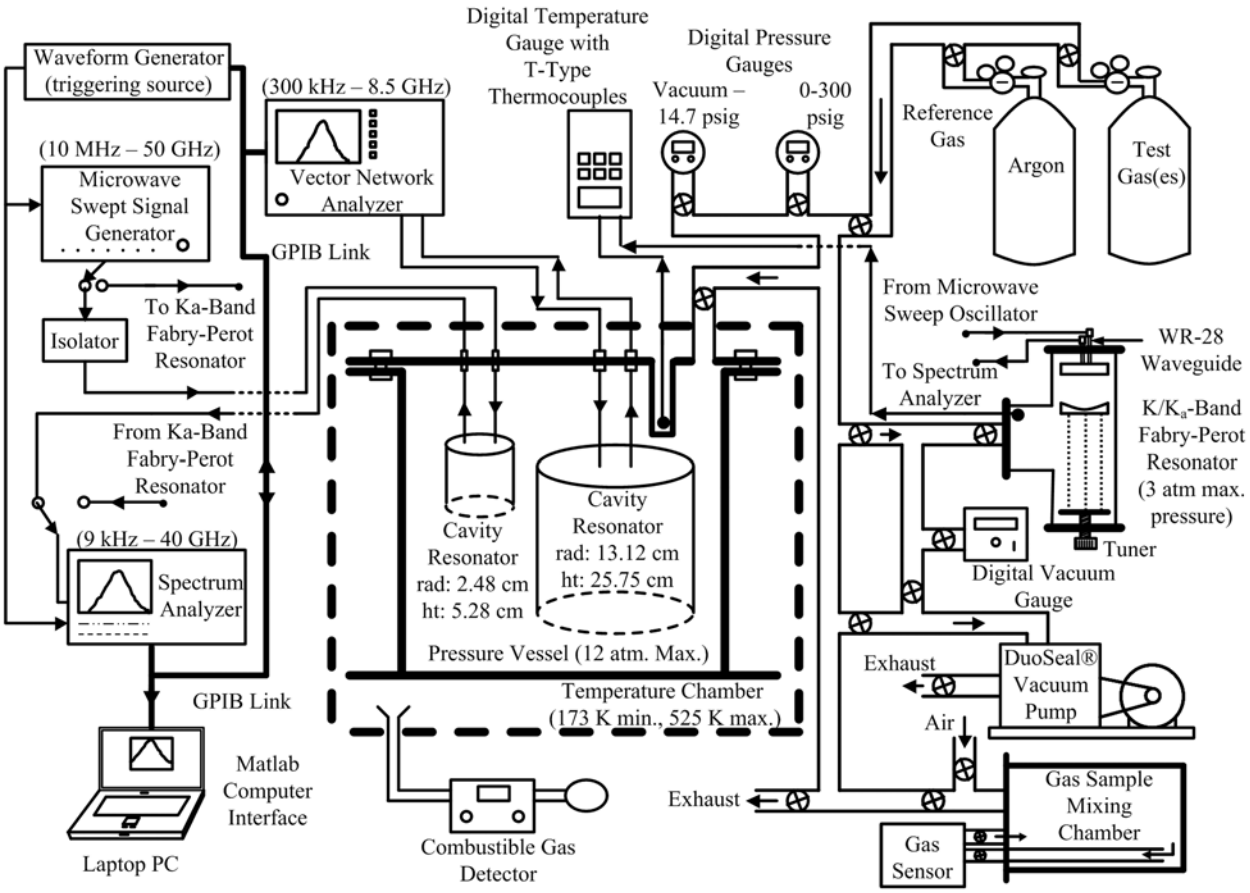

Figure 1. Block diagram of the gaseous microwave measurement system. Electrical connections are shown by solid lines with arrows displaying the direction of signal propagation. Valves controlling the flow of gases are shown by the small crossed circles.

additionally measured by another DPG7000 Digital Test Gauge with a resolution of 0.1 mbar and a 3-σ accuracy of 1.0 mbar. A Welch DuoSeal® vacuum pump Model 1376B-01 is used to evacuate the gases from the system from 1 bar down to a level of 0.1 mbar. Gases at higher pressures are ventilated through an exhaust valve. A combustible gas detector (GasTech model GP-204) can also be used to detect leaks from the pressure vessel when the system contains hydrogen. A glass tube tee capable of withstanding 3 atm of pressure is also connected to the gas handling system for mixture sampling and characterization, but is maintained at room temperature. Additionally, a glass cylinder with a volume of approximately 7.2 L is connected to the system along with an Analytical Technology, Inc. PortaSens II portable gas leak detector capable of detecting trace amounts of gases through a series of interchangeable electrochemical cartridge sensors.

3.2. Microwave Measurement Subsystem

[11] The current microwave measurement subsystem has benefited greatly by continuous improvements in the speed, accuracy, and reliability of commercially available microwave measurement devices over the past 20 years. The basics of the measurements, however, remain unchanged. At the heart of this subsystem are two stainless steel cylindrical cavity resonators positioned inside the pressure vessel. These resonators have been plated with gold, so as to improve the quality factors of their resonances, and to prevent reactions with corrosive acid vapors that have been measured in previous experiments [see, e.g., *Hanley and Steffes*, 2005]. The interior dimensions of the larger of the two resonators are 13.116 cm in radius and 25.754 cm in height, thus making it ideal for measurements from 1.5 to 8 GHz although higher frequency resonances have been measured up to 24 GHz, but with lesser accuracy. It rests at the bottom of the

pressure vessel, whereas the smaller resonator, measuring 2.484 cm in radius and 5.281 cm high (internal dimensions), rests on a shelf suspended from the top of the pressure vessel. The small resonator is best used in measurements from 13 to 25 GHz. Each resonator contains two closed-loop antenna probes mounted on their top plates and oriented to maximize the Q or quality factor of TE_{0ml} modes. The Qs for most resonances in the large resonator are around 65,000 and in the small resonator they range from 12,000 to 30,000. Both resonators are connected to hermetically sealed bulkhead feed-through connectors on the top plate of the pressure vessel, the large resonator using BNC type connectors converted to N-type at the feed-through and the small one using SMA connectors. The large resonator is connected internally using RG-142B coaxial cables and the small resonator is connected by two rigid coaxial cables with a silicon dioxide dielectric designed to withstand high temperatures. Each resonator has two horizontal slits on their circular sides near their top plates that act to suppress unwanted degenerate TM resonant modes, as well as allowing gases to enter their interiors. Additionally, the top and bottom plates of each resonator are isolated about 1.5 mm from the cylinder by a series of Teflon® washers around the connecting screws, which also increases the surface area through which gases can be exchanged between the resonator and the remainder of the vessel. This isolation essentially eliminates TE and TM modes that require currents to be flowing between the top and bottom plates and the cylinder walls including the degenerate TM_{1ml} modes. Suppressing the degenerate TM modes greatly improves the accuracy and sensitivity of the measurements.

[12] The two ports for each resonator are essentially symmetric. The feed-through ports on the pressure vessel connected internally to the large resonator are connected externally via low-loss flexible coaxial cables to a 2-port Agilent E5071C-ENA Vector Network Analyzer that operates from 9 kHz to 8.5 GHz with a high-stability timebase (Option 1E5). The feed-through ports connected to the small resonator have one port connected to an input from an HP 83650B Swept Signal Generator and the other to a high-resolution HP 8564E Spectrum Analyzer both via flexible, low-loss, high frequency coaxial cable. A number of ferrite isolators can be placed between the signal generator and the small resonator to provide a minimum of 10 dB of isolation for measurements up to 26.5 GHz. At higher frequencies, the cables themselves provide enough isolation from reflected signals due to their attenuation. All SMA connections are tightened with an 8 in-lb (0.90 N-m) torque wrench to ensure reliable connections. The detector within the spectrum analyzer operates in a positive peak mode, which displays the maximum power level received during the integration time of each point on each individual sweep. This mode is used primarily because it maximizes the data return to the computer. The normal mode detects both the high and low signal (noise floor) intensities at each frequency point, but when transferring to the computer, the spectrum analyzer is limited to 601 points in both the frequency and amplitude axes. In this mode, the peak level data becomes interspersed with the noise floor data, which would result in only half the data transferred being of practical use for these measurements and consequently would halve the frequency resolution. The network analyzer, on the other hand, offers variable and higher resolution (up to 1601 points) and does not suffer degradation due to its detection mode.

[13] The signal generator and spectrum analyzer can also be connected to a Fabry-Perot resonator contained in the glass tube tee that operates at K/K_a-band from 22 to 40 GHz. The Fabry-Perot resonator is similar to that used by *Mohammed and Steffes* [2003] and consists of two gold-plated mirrors. One mirror is flat and contains two symmetric WR-28 waveguide ports and the other mirror is concave with a focal length around 20 cm. The concave mirror is adjustable via a tuning screw and by adding standoffs between the mirror and the plate that supports it. The distance between the mirrors can be varied from 0–23 cm. However, additional resonances caused by reflections from the resonator endplates and scattering around the edges of the mirrors corrupt the spectrum when the mirrors are spaced farther apart. This places the optimum spacing somewhere between 5 and 6 cm, where the concave mirror resembles more of a flat mirror, and leads to resonances being spaced 2.5–3 GHz apart with Qs ranging from 5,700 to 13,300. The waveguides are connected to waveguide-to-coax SMA adapters, which are connected to high-frequency flexible coaxial cables. As will be discussed, this resonator can be used to verify the mixing ratio of polar molecules, such as ammonia or water vapor, contained in mixtures which may have been modified by selective adsorption of polar constituents to the walls of the large pressure vessel and cylindrical cavity resonators.

3.3. Data Handling Subsystem

[14] The data acquisition subsystem consists of a laptop computer connected to the spectrum analyzer, network analyzer, and swept signal generator via a general purpose interface bus (GPIB) connected to a National Instruments NI-488.2 interface card. The suite of instruments is controlled via Matlab® and the Standard Commands for Programmable Instruments (SCPI) and HP BASIC languages. The primary function of the software is to control the instruments and retrieve resonance data from either the spectrum analyzer or network analyzer in the form of received power as a function of frequency. Each resonance is viewed with the amplitude axis extending over a 10 dB range and with the frequency

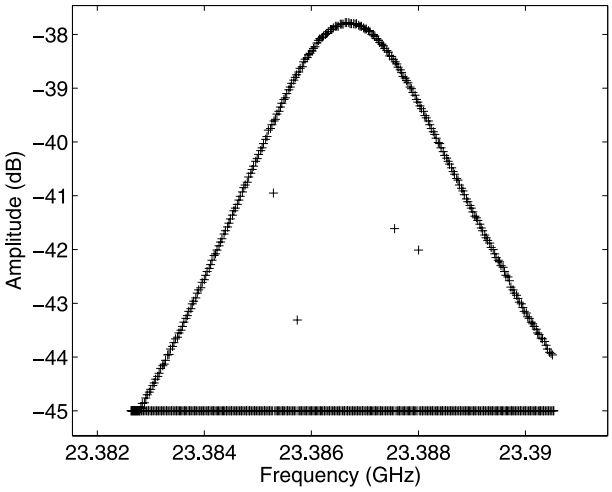

Figure 2. Spectrum analyzer output of a resonance in the Fabry-Perot resonator with a 40 s sweep time. The large number of data points at −45 dB result from sweep-on-scan nulls. The four intermediate valued points are the result of partial overlap of the swept signal with the spectrum analyzer's Gaussian detector.

axis being approximately twice the half-power bandwidth. This ''zooming-in'' on each resonance allows the best resolution without spreading the resonance over multiple screen widths. The resolution bandwidth (RB) of the spectrum analyzer is set to the value closest to 1/100th of frequency span of a particular resonance under the resonance's broadest condition during the experiment. The value of RB is limited to 1 or 3 times any integer power of ten within the specifications of the device and is kept constant for all measurements of a specific resonance. The video bandwidth (VB) is set to 1/10th of the resolution bandwidth, to provide some filtering of the signal. The software used is similar to the PCSA program created by *DeBoer and Steffes* [1996] but with the added flexibility of Matlab® and the ability to process the incoming data to directly calculate absorptivity and refractivity along with storing all raw data sets.

[15] One problem that arises with the measurements taken using the spectrum analyzer is due to sweep-on-scan nulls. When it is not possible to synchronize the swept signal generator to the spectrum analyzer, the signal generator is set to sweep at a fast pace while the spectrum analyzer is set at a slower rate. The sweep rate for the signal generator is set at 75 ms at which the device can put out a stable power level at all frequencies used. It can be made to sweep as fast as 10 ms, but the detected signal is noisier. Although the sweep time is 75 ms per sweep, there can be up to a 100 ms delay between individual sweeps, depending on the frequency. In order for the spectrum analyzer to detect the signal in each measurement bin reliably, there must be a dwell time of at least ∼175 ms during each of the 601 frequency measurement bins, which would require nearly 2 min per sweep. For each resonance measurement it is beneficial to take multiple sweeps to decrease variance, so it is optimal to have shorter, more frequent sweeps and to use the computer to average the results. If we limit the amount of time for each measurement to 200 s, the standard deviation of the set of measurements weighted by the statistical confidence coefficient seems to be minimized for 5 sweeps of 40 s each. The data from each set of sweeps is saved in a unique file. An example plot of the raw data from one of these sweeps can be seen in Figure 2.

[16] To utilize the data taken with the spectrum analyzer, the points where the input signal was not fully detected must be filtered out. Most of the time, the value of these points is equal to the baseline noise power of the measurement range and allows for easy filtering. However, because the input power is a swept Gaussian signal, there are times where the peak of the input signal is not detected within the resolution bandwidth of a data point, but some fraction of the signal is. These erroneous data points are more difficult to remove because their behavior is less predictable. To compensate for this, an algorithm is run to fill in all 601 data points as though they detected the peak of the swept input signal. The algorithm sets the value of each point equal to the average of the four nearest points (two higher and two lower) if it is less than that average. For the points within two of either end, the average is done on fewer than four points to avoid the curve being leveled at the edges. This is done until an iteration is reached where the change at every point is less than 0.01% or a maximum number of iterations has been reached, in this case 15. This corrects all the original null points but does not account for noisy spikes that stand above the good data. To compensate for these, the same algorithm is used, except that it only changes points that are greater than the average of the four nearest points until the change is less than 5% or a maximum of 10 iterations. Finally the data are smoothed once more with another four-point averaging filter where every point is set equal to the 4-point average until the change is less than 0.1% or a maximum of 5 iterations. This method, however, does not accurately measure the peak value of the resonance, especially in cases where the half power bandwidth is very narrow relative to the span. An averaging filter such as this would tend to level the data and if run through enough iterations, would eventually turn it into a horizontal line. Instead, this algorithm is merely used to detect which of the original 601 points received the peak power of the swept signal source by comparing the original data to the data from the algorithm and excluding the points where the differ-

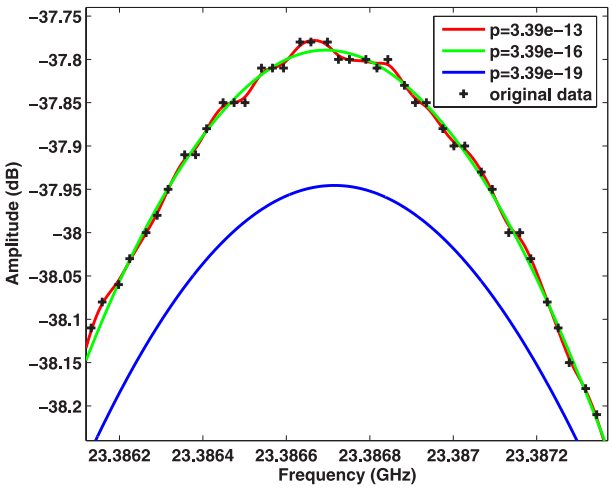

Figure 3. A close-up of the same data as Figure 2 fitted with the cubic smoothing spline, using various smoothing parameters (p). As p goes to zero, the smoothed data become a straight line equivalent to a linear regression across the data set. The value of p used in the data processing is typically the default value calculated by Matlab (shown in red), divided by 10^3 or 10^4, as determined by limiting the overall average change in the peak amplitude to 0.02 dB.

ence between the two is greater than 0.1 dB. Note that the number of valid data points is typically between 200 and 250 of the 601 points returned by the spectrum analyzer in one sweep due to the sweep-on-scan effects.

[17] A cubic smoothing spline (Matlab® function *csaps* or Fortran *SMOOTH* [*de Boor*, 2001]) with a relatively high smoothing factor is used to create a piecewise polynomial function to represent the valid data from the spectrum analyzer, or any data taken by the network analyzer (which does not suffer from sweep-on-scan nulls). This allows a mathematically precise estimate of the peak value of the resonance and the corresponding 3-dB points. A sample plot of the data fitted with smoothing splines using various smoothing parameters is shown in Figure 3. The software calculates the center frequency, half-power bandwidth, power level at the peak, asymmetry, and Q of each sweep and produces results for the mean and standard deviation of those values to another program which utilizes all the data taken during an experiment to calculate the measured absorptivities and refractivities and their corresponding uncertainties.

[18] When it is possible to synchronize the swept signal generator with the spectrum analyzer, much greater resolution can be obtained, and much faster sweep times may be used. The measurements taken with the network analyzer are much quicker and require less processing. The network analyzer is capable of generating 60 synchronized data sweeps in a single second at 1601 points of resolution. These 60 sweeps (30 each of S12 and S21) are saved to the laptop and then undergo the same processing to calculate the average and standard deviation of the center frequency, half-power bandwidth, power level, asymmetry, and Q.

4. Measurement Procedure

[19] The first step of any experiment is to make sure the gas handling system is sufficiently leak-proof. Any major leaks will add to the uncertainty of the experiment and in the case of toxic or flammable gases present a health hazard. The most difficult component to seal is the pressure vessel. The top is tightened with up to 350 ft-lbs of torque on the large bolts at room temperature before it is placed in the temperature chamber. For warm experiments, the expansion of the metal creates a better seal, but the contrary is true at colder temperatures. For cold experiments the vessel is cooled to −55°C, the warmest temperature the freezer can maintain, and then it is removed from the freezer and immediately tightened again. Although the seal on the vessel is worse at experiments conducted as cold as −100°C any attempt to tighten the vessel at these temperatures could crack the Viton® O-ring. Additional tightening of the pressure vessel is performed with the vessel evacuated, which, given the approximately 200 square inches of surface area on its top plate, lends an additional 3000 lbs of compression force due to normal atmospheric pressure. Any leaky connections throughout the gas-handling system are detected at higher positive pressures using a soap-water solution to create bubbles.

[20] With the system sealed, a series of experiments can be performed. A typical experiment consists of characterizing a gas or gas mixture at a fixed temperature across a range of frequencies for various pressures. Owing to the large thermal constant of the system, changing temperatures during an experiment is too time consuming and impractical. This also allows for smaller temperature fluctuations (typically no more than 1°C) throughout the duration of an experiment. Changes in pressure can cause slight changes in temperature as well as mixing ratio in the case of mixtures where some components adsorb and desorb more than others. This means that significantly changing pressures (more than ± 100 mbar) requires allowing the system time to stabilize for anywhere from an hour to almost a day depending on the magnitude of the pressure change and the temperature of the experiment. The convenience of the network analyzer, signal generator, and spectrum analyzer make changing measurement frequencies almost instantaneous. Therefore, it becomes most efficient to measure a number of resonances once the system has stabilized at a

Table 1. Surface Areas and Volumes for the Various Regions Inside the Pressure Vessel

	Volume, cm^3	Surface Area, cm^2	SA/V Ratio
Small resonator	102	117	1.14
Large resonator	13,919	3179	0.23
Remainder of vessel	~18,000	~9000	~0.50

specific temperature and pressure (TP). To ensure TP stabilization and thorough mixing of the gas(es) throughout the test chambers, the Qs of a number of resonances are monitored from the beginning of any pressure modification until the change in Q with respect to time (dQ/dt) is essentially zero. This method is most accurate when small changes in temperature and mixing ratio measurably affect the microwave opacity, or in the pressure vessel where the mixing ratio of the gas in the small cylindrical cavity resonator is not yet equal to that in the large cylindrical cavity resonator.

[21] When trying to characterize the pressure-broadening effects of one or more lossless gases on the opacity of a microwave absorbing gas, it is necessary to measure a mixture of the gases, since intermolecular collisions cannot always be accurately theoretically characterized. Certified gas mixtures can be ordered to fairly accurate specifications through most major gas suppliers, but if the goal of a series of experiments is to characterize the effects of different concentrations of the individual components, then it becomes more practical to use cylinders of pure gases and mix them in the measurement system using the pressure gauges to measure the amounts of each gas. When dealing with gases that have a strong tendency to adsorb to surfaces, such as molecules with a large dipole moment (i.e., H_2O and NH_3), certain precautions must be taken to ensure accurate production of a mixture. Since the abundances of typical microwave absorbers such as NH_3, H_2O, H_2S, SO_2 and PH_3 are usually much less than 1% in planetary atmospheres, realistic characterization (provided the opacity exceeds the sensitivity of the system) places the mole fraction of any one of these gases in the minority. This means that adsorption of these components can have drastic effects on the measurements if not properly accounted for.

[22] For example, as a mixture of ammonia, hydrogen, and helium is added to the pressure vessel, it migrates through inlet gaps into the two cavity resonators. The surface-to-volume ratio of the pressure vessel and the two resonators are each different, as in Table 1. Thus, the time scales for reaching a stable mixing ratio throughout the two resonators and within the pressure vessel itself vary significantly. Since the large resonator has the smallest surface-to-volume ratio, it initially encounters less ammonia adsorption (and therefore a higher ammonia mixing ratio, indicated by a lower quality factor of its resonances). By monitoring the quality factor of the resonator, it is possible to determine the time scale of the mixing process within the multiresonator system whereby a uniform mixing ratio is reached. As shown in Figure 4, mixing ratio equilibration in the large resonator occurs over a period of approximately 15 hours.

[23] In the small resonator, the strong effect of the adsorption of ammonia is visible during the first hour after the gas mixture is introduced, as shown in Figure 5. However, once the sites on the metallic surface are occupied, no additional adsorption occurs. As equilibrium is reached with the gas contained in the remainder of the pressure vessel (where adsorption is less significant), the mixing ratio of ammonia rises (resulting in a lower quality factor).

[24] The best way to create mixtures with small amounts of adsorbing constituents is to add those constituents to the system first and allow them to saturate the surfaces where they adsorb until equilibrium is reached between the amount of gas adsorbed, the surface coverage of the adsorption, and the partial pressure of the remaining adsorbate gas. At this point the rates of adsorption and desorption are equal. Although the ma-

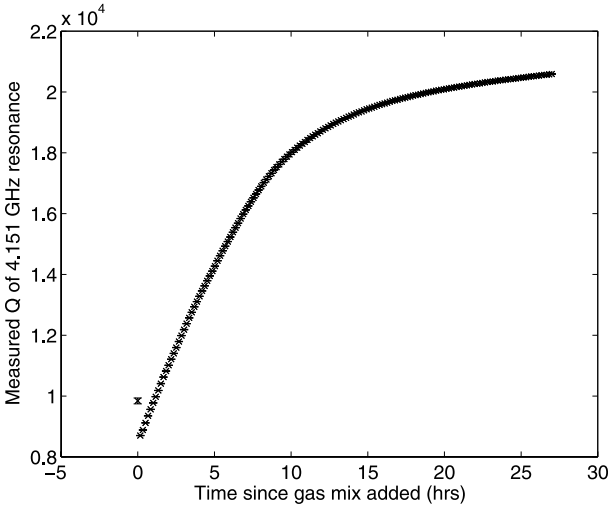

Figure 4. Measured Q of 4.151 GHz resonance in the large cylindrical cavity resonator as a function of time after a mixture of ~1% NH_3, 13.5% He, and 85.5% H_2 has been added to the pressure vessel at a temperature of 216 K. The increasing Q is due to the lessening of the opacity of the mixture caused mainly by two factors: the microwave absorber (NH_3) adsorbing or adhering to the sides of the test chambers and more thorough mixing of the gas between the two resonators and the remainder of the pressure vessel.

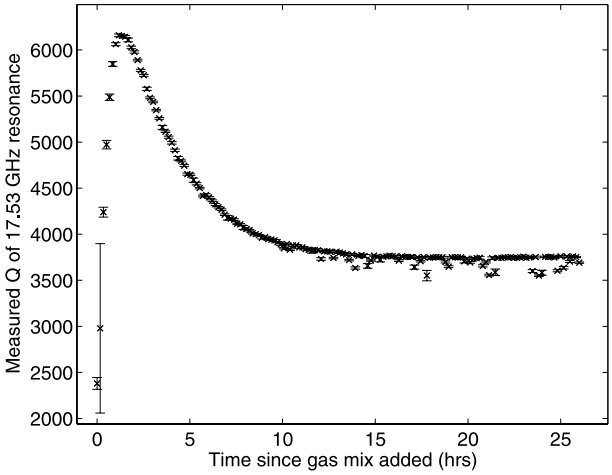

Figure 5. Measured Q of 17.53 GHz resonance in the small cylindrical cavity resonator as a function of time after a mixture of ~1% NH_3, 13.5% He, and 85.5% H_2 has been added to the pressure vessel. The sharp rise in Q results from NH_3 adsorption in the small resonator, whereas the accompanying decrease is caused by mixing throughout the vessel where the NH_3 concentration is greater.

jority of the adsorption occurs within the first few minutes, the gas can continue to adsorb up to 20 hours after admission to the system depending on the pressure of the gas and the texture of the adsorbent surfaces. Once equilibrium is reached at the desired pressure of the adsorbing gas, additional gases are added until the maximum total pressure is reached (usually 3, 6, or 12 bars depending on the experiment). Additional lower pressures are achieved by venting or vacuuming the gas mixture from this point.

[25] The uncertainty in knowledge of the mole fractions of each gas can be directly mapped to the uncertainty of the pressure or vacuum gauge used to measure each component. The greatest uncertainty usually lies in the mole fraction of the least abundant component. One way of reducing this is to create a mixture with a larger concentration of that component and then perform a series of dilutions. Unfortunately, if any of the constituents are strong adsorbers, diluting the mixture would cause a shift in the adsorption/desorption equilibrium since the partial pressure of that gas would decrease. This would lead to additional desorption and disproportionately increase the concentration of that gas. Therefore dilution can only be performed with nonpolar gases. The desorption that occurs with a drop in partial pressure means that the measured mixing ratio at the original highest pressure will be less than that at lower pressures. To measure these mixing ratios in experiments performed in the pressure vessel, a small gas sample is drawn into the Fabry-Perot resonator and characterized from 22–40 GHz at 6 or 7 resonances. These data can be compared to those taken with known concentrations, or calculated using a model, provided an accurate one exists. Although the Fabry-Perot resonator is maintained at room temperature and is mostly glass, significant adsorption can still occur even there. Whether this occurs exclusively on the metallic surfaces (mirrors, end plates, standoffs, and waveguides), on the glass (Pyrex®), or both is not completely known. In order to compensate for this adsorption, a gas sample is introduced and allowed to equilibrate (adsorb), then half is removed and replaced with a fresh sample. This is repeated three or four times until the dQ/dt of the resonances in the Fabry-Perot resonator is no longer significant. At this point, the concentration of each gas in the pressure vessel is essentially equal to that in the Fabry-Perot resonator and the characterization from 22–40 GHz can be performed. If the goal of the experiment if to use the Fabry-Perot resonator as the primary measurement tool, then a mixture is created at a higher pressure (6–12 bars) in the pressure vessel as previously described. This mixture can then be vented into the Fabry-Perot resonator and measured starting with the lower pressures and increasing, each time using the replace half technique to compensate for adsorption in the Fabry-Perot system. This works without significant desorption in the pressure vessel because its volume is approximately 8 times that of the Fabry-Perot system, so the overall pressure change is relatively small. Nonetheless, it is best to measure the lower pressures of an experiment in the Fabry-Perot resonator first and then the higher pressures.

[26] After the gas or gas mixture has been measured at all the desired pressures of an experiment, a vacuum is drawn and the system is flushed a number of times with argon over a period of a few days to ensure any adsorbed gases are removed so that when dielectric matching is performed, the gas present, argon, is lossless and does not contain any desorbed lossy gases. To double check that this is the case, argon is added to the system and allowed to stand for a minimum of six hours. It is then drawn into the evacuated detection chamber to a level of a half-bar and mixed with ambient air to provide the minimum 5% O_2 required by the electrochemical sensor cell. This gas is continuously circled through the detector and the level of the adsorbate gas is measured in parts per million (ppm). Once the threshold of gas detection can no longer be reached, the system is considered purged. As an added precaution, argon that is used during dielectric matching is not allowed to stand in the system for more than 6 hours without being replaced with fresh argon from the cylinder tank.

[27] Before any gases are added to the system, all the resonances of the system are measured under vacuum to

create a baseline. After the test gas(es) have been measured and the system has been purged, a second vacuum measurement is performed along with measuring the straight-through transmissivities of the cables in the system under the same conditions (i.e., center frequency, span, RBW, etc.) as in each pressure/frequency point of the test gas(es). The transmissivity measurements consist of multiple sweeps for each resonance and are measured two more separate times before the end of the experiment to better statistically characterize the reproducibility of the electrical connections. The frequency that each resonance shifted to while the system was loaded with the test gas is calculated and argon is added until each resonance has shifted to that same frequency and a dielectrically matched measurement is taken. This usually requires a slightly different pressure of argon for each resonance depending on the structure of the absorption spectrum of the gas(es). After the end of the dielectric matching, a third vacuum measurement is performed to check that the Qs of each resonance have returned to their preexperiment values.

5. Data Processing

[28] The data processing begins after an experiment has been completed. Software was created that loads the experimental data, runs the smoothing algorithms, and calculates the absorptivity and refractivity of the test gas at the measured frequencies, pressures, temperature and mole fraction. Any major variation in cable transmissivity over the frequency range of a resonance is deconvolved from the measured sweeps. The transmissivity of the cables at the frequency of each resonance under each pressure condition is calculated by averaging the values of the average of each set of sweeps from the three transmissivity measurements. This value is subtracted from the peak power measured from the test gas and matching gas and the result is the insertion loss (S). The first and last vacuum measurements are compared to the middle one for consistency, but the values of the middle vacuum measurement are used most because they are temporally closest to the loaded and matched measurements.

[29] There are five uncertainties for any measurement in this system: instrumentation errors and electrical noise (σ_n), errors in dielectric matching (σ_{diel}), errors in transmissivity measurement (σ_{trans}), errors due to resonance asymmetry (σ_{asym}), and errors in measurement conditions (σ_{cond}) resulting from uncertainty in temperature, pressure and mixing ratio. The instrumentation and electrical noise error results from the sensitivity of the electrical devices used and their accuracy in measuring center frequency and bandwidth. It is calculated as in the work of *Hoffman et al.* [2001], but with the addition of the network analyzer's frequency sensitivity. The dielectric matching error results from imperfect dielectric matching and is also calculated as in the work of *Hoffman et al.* [2001]. The error in transmissivity is calculated by using the standard deviation of the three means of the transmissivity measurements weighted by the 95% confidence coefficient 4.303 divided by the square root of the number of samples, or $\sqrt{3}$ in this case. This roughly 2-σ uncertainty is propagated through equation (7) to calculate a maximum and minimum value for opacity. The error in transmissivity (σ_{trans}) is then set as half the difference between these maximum and minimum values for α. The asymmetry error is calculated by dividing each resonance in half and calculating two opacities based on 3-dB bandwiths calculated as

$$BW_h = 2 \times (f_h - f_c) \tag{11}$$

$$BW_l = 2 \times (f_c - f_l) \tag{12}$$

where BW_h and BW_l are the bandwidths of the high and low sides of the resonance, respectively. The difference between the opacities calculated with these bandwidths is essentially treated as a 2-σ asymmetry error. Because some of these errors can be systematic, the overall 2-σ uncertainty for any data point is given by the sum of the respective standard deviations:

$$\sigma_{Total} = \sigma_n + \sigma_{diel} + \sigma_{trans} + \sigma_{asym}. \tag{13}$$

The dominant uncertainty in most cases is σ_{trans}, except in cases of somewhat asymmetric resonances (A > 1) where σ_{asym} tends to dominate. Although not directly affecting the opacity measurements, the measured uncertainty in temperature, pressure and mixing ratio (σ_{cond}) factors into creating accurate models for opacity based on the experimental results. To quantify this uncertainty in terms of opacity, the temperature (T), pressure (P), and concentration (C) dependences on modeled opacity must be fairly well known. Because this is not often the case, σ_{cond} is maintained separate from σ_{total}. If the T, P, and C dependences are known, then the maximum and minimum modeled opacities for each variation (T, P, and C) are calculated and the uncertainty of each is set to half the difference of maximum and minimum. Then

$$\sigma_{cond} = \sigma_T + \sigma_P + \sigma_C, \tag{14}$$

where σ_T, σ_P, and σ_C are the model uncertainties in temperature, pressure, and concentration, respectively. For refractivity, the sensitivity reflects electrical uncertainties in measurement of the center frequencies of the resonances being measured. The system sensitivities for absorption and refraction measurements are shown in Table 2 along with a breakdown of the comparative effects of each uncertainty in Table 3. As one example of

Table 2. Some Sample Absorption and Refraction System Sensitivities at Various Resonant Frequencies

Frequency, GHz	TE Mode, n,m,l	2-σ Absorptivity Sensitivity, dB/km	2-σ Refractivity Sensitivity, unit-less
	Large Cylindrical Cavity Resonator		
1.51	0, 1, 1	0.01	0.050
2.25	0, 1, 3	0.01	0.075
3.76	0, 1, 6	0.02	0.125
5.99	0, 1, 10	0.04	0.198
	Small Cylindrical Cavity Resonator		
14.62	0, 2, 2	0.05	1.31
19.75	0, 3, 1	0.25	1.46
22.60	0, 3, 4	0.5	2.46
24.15	0, 3, 5	1.0	3.08
	Fabry-Perot Resonator		
23.39	0, 1, 9	1.0	3.95
25.95	0, 1, 10	0.5	3.58
28.52	0, 1, 11	0.25	2.46
33.64	0, 1, 13	0.75	2.01

the impact of improved sensitivities, earlier versions of the measurement system [*Steffes and Jenkins*, 1987] were not accurate enough to discriminate between four models for ammonia opacity, whereas the current system is, as evidenced by Figure 6. The effects of temperature, pressure, and concentration uncertainty can be seen in the double lines for each model and show how σ_{cond} compares to σ_{total} in this case.

6. Future Improvements

[30] Although this system is capable of making high-accuracy measurements of the microwave properties of gases, there are plans to extend its available frequency and pressure ranges. A glass-envelope confocal Fabry-Perot resonator has been newly developed to allow measurements from 75–120 GHz at pressures up to 3 bars. To generate signals in this range, a times-six active multiplier chain will be used, whereas a harmonic mixer locked to the 18th harmonic will be used with the spectrum analyzer as a signal detector. Another upgrade to the system will be the addition of a pressure vessel

Table 3. A Breakdown of the Percentage Contributions of Each Uncertainty on σ_{total} for a Typical Experiment

Frequency, GHz	1.51	5.99	14.62	22.60	23.39	33.64
σ_n, %	2.3	0.21	10.2	4.73	24.9	2.97
σ_{diel}, %	0.05	0.01	0.30	0.02	0.30	0.02
σ_{trans}, %	97.3	62.8	24.4	7.17	20.6	61.0
σ_{asym}, %	0.35	37.0	65.1	88.1	54.2	36.0

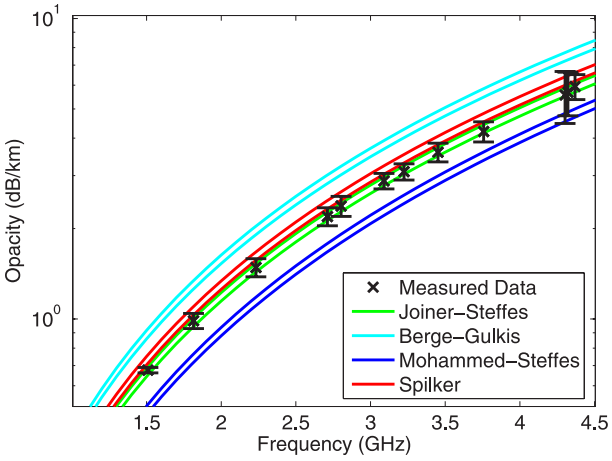

Figure 6. Recent data from the present microwave measurement system on the opacity of gaseous ammonia (0.83% mole fraction) in a hydrogen (85.68%) and helium (13.49%) atmosphere at a pressure of 6.02 bars and temperature of 295 K plotted along with their error bars (σ_{total}). Also shown are four commonly used models for H_2/He-broadened NH_3 opacity: *Joiner and Steffes* [1991], *Berge and Gulkis* [1976], *Mohammed and Steffes* [2003], and *Spilker* [1990]. The double lines represent the range of values the models have due to measurement uncertainty in temperature, pressure and NH_3 concentration (σ_{cond}).

capable of withstanding pressures up to 100 bars containing either a cylindrical cavity or Fabry-Perot resonator. Future improvements could be made by extending the frequency range measurable by network analyzer up to 40 GHz or possibly even higher. This would allow greater precision in this range along with shorter measurement times. We have been able to obtain a 50 MHz to 40 GHz network analyzer (HP 8722D) for limited times from colleagues to verify these potential improvements.

7. Conclusion

[31] The High-Sensitivity Microwave Measurement System described has evolved greatly from its first configurations where the measurement sweeps were read on the spectrum analyzer by eye. The sensitivities have vastly improved in response to a demand for more precise radiative transfer models and with more accurate equipment. The measurement procedure has also become more complicated and time-consuming to allow this greater precision. System upgrades evolving from technological improvements will continue to be implemented as time and money allow. Regardless of the specifics of

the system, it will continue to provide accurate and precise measurements of the microwave properties of various gases long into the future.

[32] **Acknowledgments.** This work is supported by the NASA Planetary Atmospheres Program under grant NNG06GF34G. Additional support has been provided by NASA under contract 699054X from the Southwest Research Institute supporting the Juno Mission Science Team. The authors wish to thank G. Durgin, W. Doolittle, and C. Kautz for their contributions to system upgrades.

References

Berge, G. L., and S. Gulkis (1976), Earth-based radio observations of Jupiter: millimeter to meter wavelengths, in *Jupiter*, edited by T. Gehrels, pp. 621–692, Univ. of Ariz. Press, Tucson.

Bleaney, B., and J. H. N. Loubser (1950), The inversion spectra of NH_3, CH_3Cl and CH_3Br at high pressures, *Proc. Phys. Soc., Sect. A.*, *63*, 483–493.

DeBoer, D. R., and P. G. Steffes (1994), Laboratory measurements of the microwave properties of H_2S under simulated Jovian conditions with an application to Neptune, *Icarus*, *109*, 352–366.

DeBoer, D. R., and P. G. Steffes (1996), The Georgia Tech high sensitivity microwave measurement system, *Astrophys. Space Sci.*, *236*, 111–124.

de Boor, C. (2001), *A Practical Guide to Splines, Revised Edition*, Springer, New York.

Hanley, T. R., and P. G. Steffes (2005), Laboratory measurements of the microwave opacity of hydrochloric acid vapor in a carbon dioxide atmosphere, *Icarus*, *177*, 286–290, doi:10.1016/j.icarus.2005.03.018.

Ho, W., I. A. Kaufman, and P. Thaddeus (1966), Laboratory measurements of microwave absorption in models of the atmosphere of Venus, *J. Geophys. Res.*, *71*, 5091–5108.

Hoffman, J. P., P. G. Steffes, and D. R. DeBoer (2001), Laboratory measurements of the microwave opacity of phosphine: opacity formalism and application to the atmospheres of the outer planets, *Icarus*, *152*, 172–184.

Joiner, J. (1991), Millimeter-wave spectra of the Jovian planets, Ph.D. thesis, Georgia Inst. of Technol., Atlanta.

Joiner, J., and P. G. Steffes (1991), Modeling of Jupiter's millimeter wave emission utilizing laboratory measurements of ammonia (NH3) opacity, *J. Geophys. Res.*, *96*, 17,463–17,470.

Kolodner, M. A., and P. G. Steffes (1998), The microwave absorption and abundance of sulfuric acid vapor in the Venus atmosphere based on new laboratory measurements, *Icarus*, *132*, 151–169.

Matthaei, G. L., L. Young, and E. Jones (1980), *Microwave Filters, Impedance Matching Networks and Coupling Structures*, McGraw-Hill, New York.

Mohammed, P. N. (2005), Laboratory measurements of the millimeter wavelength opacity of phosphine (PH_3) and ammonia (NH_3) under simulated conditions for the Cassini-Saturn encounter, Ph.D. thesis, Georgia Inst. of Technol., Atlanta.

Mohammed, P. N., and P. G. Steffes (2003), Laboratory measurements of the Ka-band (7.5 to 9.2 mm) opacity of phosphine (PH_3) and ammonia (NH_3) under simulated conditions for the Cassini-Saturn encounter, *Icarus*, *166*, 425–435, doi:10.1016/j.icarus.2003.09.003.

Morris, E. C., and R. W. Parsons (1970), Microwave absorption by gas mixtures at pressures up to several hundred bars. I. Experimental technique and results, *Aust. J. Phys.*, *23*, 335–349.

Spilker, T. R. (1990), Laboratory measurements of the microwave absorptivity and refractivity spectra of gas mixtures applicable to giant planet atmospheres, Ph.D. thesis, Stanford Univ., Stanford, Calif.

Steffes, P. G., and V. R. Eshleman (1981), Laboratory measurements of the microwave opacity of sulfur dioxide and other cloud-related gases under simulated conditions for the middle atmosphere of Venus, *Icarus*, *48*, 180–187.

Steffes, P. G., and J. M. Jenkins (1987), Laboratory measurements of the microwave opacity of gaseous ammonia (NH3) under simulated conditions for the Jovian atmosphere, *Icarus*, *72*, 35–47.

Tyler, G. L., and H. T. Howard (1969), Refractivity of carbon dioxide under simulated Martian conditions, *Radio Sci.*, *4*, 899–904.

T. R. Hanley and P. G. Steffes, School of Electrical and Computer Engineering, Georgia Institute of Technology, 777 Atlantic Drive, Atlanta, GA 30332-0250, USA. (gtg237n@mail.gatech.edu; ps11@mail.gatech.edu)